Rapid loss of motor nerve terminals following hypoxia-reperfusion injury occurs via mechanisms distinct from classic Wallerian degeneration

Journal of Anatomy

J. Anat. (2008) **212**, pp827–835 doi: 10.1111/j.1469-7580.2008.00909.x

Rapid loss of motor nerve terminals following hypoxia–reperfusion injury occurs via mechanisms distinct from classic Wallerian degeneration

Becki Baxter,[1] Thomas H. Gillingwater[1,2] and Simon H. Parson[1]

[1]*Centre for Integrative Physiology and* [2]*Centre for Neuroscience Research, School of Biomedical Sciences, University of Edinburgh, Old Medical School, Edinburgh, UK*

Abstract

Motor nerve terminals are known to be vulnerable to a wide range of pathological stimuli. To further characterize this vulnerability, we have developed a novel model system to examine the response of mouse motor nerve terminals in *ex vivo* nerve/muscle preparations to 2 h hypoxia followed by 2 h reperfusion. This insult induced a rapid loss of neurofilament and synaptic vesicle protein immunoreactivity at pre-synaptic motor nerve terminals but did not appear to affect post-synaptic endplates or muscle fibres. The severity of nerve terminal loss was dependent on the age of the mouse and muscle type: in 8–12-week-old mice the predominantly fast-twitch *lumbrical* muscles showed an 82.5% loss, whereas the predominantly slow-twitch muscles *transversus abdominis* and *triangularis sterni* showed a 57.8% and 27.2% loss, respectively. This was contrasted with a > 97% loss in the predominantly slow-twitch muscles from 5–6-week-old mice. We have also demonstrated that nerve terminal loss occurs by a mechanism distinct from Wallerian degeneration, as the slow Wallerian degeneration (*Wld*^{S}) gene did not modify the extent of nerve terminal pathology. Together, these data show that our new model of hypoxia–reperfusion injury is robust and repeatable, that it induces rapid, quantitative changes in motor nerve terminals and that it can be used to further examine the mechanisms regulating nerve terminal vulnerability in response to hypoxia–reperfusion injury.

Key words ischaemia; neuromuscular junction; selective vulnerability; synapse, *Wld*^{S}.

Introduction

There is a growing body of evidence showing that nerve terminals throughout the nervous system are vulnerable to a range of traumatic, toxic and disease-related neurodegenerative stimuli (reviewed in Wishart et al. 2006). One such pathological stimulus is ischaemia/ hypoxia and whereas this has been extensively studied in the central nervous system (CNS), surprisingly few studies have addressed its effects in the peripheral nervous system (PNS). This is despite the fact that the peripheral nervous system can be highly susceptible to reductions in blood supply, and therefore oxygen levels, during surgical and pathological conditions. For example, approximately 1 million procedures annually in the USA utilize surgical and non-surgical tourniquets (McEwen, 1981). These are most commonly used to create bloodless surgical fields, particularly in orthopaedic and plastic surgery but also for the administration of intravenous regional anaesthesia and for manipulation of blood pressure. Without proper consideration of tourniquet design, pressure, application time and local anatomy, tourniquet use can cause long-term injury (for reviews see McEwen, 1981; McGraw & McEwen, 1987; Kam et al. 2001). The most common complications, affecting more than 60% of surgical patients (Saunders et al. 1979), are neurological and range from mild functional loss through to complete limb paralysis and permanent functional deficits (Rorabeck, 1980). It is far from clear what aspect of tourniquet application leads to these observed neurological deficits, as it is well accepted that tourniquets not only restrict blood flow but also cause mechanical trauma to underlying peripheral nerves (Ohara et al. 1996; Kam et al. 2001). Several groups have suggested that tourniquets cause injury to distal motor nerve terminals (Makitie & Teravainen, 1977; Hatzipantelis et al. 2001; Tombol et al. 2002; Eastlack et al. 2004; David et al. 2007), whereas skeletal muscle appears structurally and functionally spared (Makitie & Teravainen, 1977; Hatzipantelis et al. 2001; Tombol et al. 2002; Eastlack et al. 2004; David et al. 2007). Hypoxia is considered to be the key pathological

Correspondence
Dr Simon H. Parson, Section of Anatomy, Old Medical School, Teviot Place, University of Edinburgh, Edinburgh, EH8 9AG, UK. T: +44 (0)131 6503552; E: s.h.parson@ed.ac.uk

Accepted for publication *20 March 2008*

stimulus in CNS ischaemia (Bickler & Donohoe, 2002) and other groups have shown that hypoxia can induce functional changes at the neuromuscular junction (Nishimura, 1986; Bukharaeva et al. 2005).

The mechanisms underlying nerve terminal vulnerability to hypoxia–reperfusion injury in situations such as tourniquet-induced ischaemia–reperfusion remain unclear (David et al. 2007). The development of robust, experimentally accessible models for quantitative study is therefore required. Most current *in vivo* animal models of hypoxia–reperfusion rely on the experimental application of elasticated rubber bands as high-pressure tourniquets. Such approaches may induce considerable mechanical stress and potential crush injury to underlying nerves, making it difficult to conclusively distinguish the effects of ischaemia–reperfusion injury from the effects of mechanical trauma. Only one study has suggested that peripheral nerve injury occurs independently of the mechanical trauma associated with tourniquets (Hatzipantelis et al. 2001).

Here we report the development of a novel, quantitative *ex vivo* model of hypoxia–reperfusion injury that allows us to model hypoxic injury independent of confounding factors such as glucose depletion, biochemical changes, mechanical trauma and others. We use this experimental model to show that motor nerve terminals in different skeletal muscles are vulnerable to 2 h hypoxia followed by 2 h reperfusion. We show age-related differences in synaptic vulnerability and also demonstrate that motor nerve terminal pathology occurs via a mechanism distinct from classic Wallerian degeneration.

Methods

Animals

Tissue was obtained from 5–12-week-old female C57Bl/6 mice or 5–6-week-old female C57Bl6/Wlds mice (all obtained from Harlan-Olac, UK) culled by cervical dislocation in accordance with the Animal (Scientific Procedures) Act 1986. Skeletal muscles with distal nerve stumps were quickly dissected in a silicone (Sylgard 184: Dow Corning, Germany) lined Petri dish and maintained in HEPES buffered Krebs' solution (144 mM Na^+, 5 mM K^+, 2 mM Ca^{2+}, 1 mM Mg^{2+}, 131.2 mM Cl^-, 23.8 mM HCO^{3-}, 0.4 mM $H_2PO_4^{2-}$, 5 mM D-glucose, 5.5 mM HEPES: pH 7.2–7.4) and sparged with 95% : 5% O_2 : CO_2 gas. Skeletal muscles were selected because their anatomy minimized diffusion distances. Preparations consisted of the four deep *lumbrical* muscles (attached to the tendon of *flexor digitorum longus*) with a long sciatic/tibial nerve stump, *transversus abdominis* (TA) or *triangularis sterni* (TS), with intact intercostal nerve stumps, from the deep surface of the abdominal and thoracic walls, respectively. Care was taken to ensure that all muscles were free of dissection damage and that their nerve supply remained intact to protect against injury-induced Wallerian degeneration (Waller, 1850; Miledi & Slater, 1970). As the lumbrical muscles and their long nerve stump are particularly vulnerable to dissection damage, we verified their integrity before use in experiments by stimulation with a suction electrode. Where tested, all muscles produced a twitch response at 0.5 V or below.

Hypoxia–reperfusion

HEPES buffered saline 250 mL was vigorously sparged with 95% : 5% N_2 : CO_2 for a minimum of 1.5 h in a 250-mL conical flask prior to the start of experimentation. The long setup period was required to ensure maximum displacement of already dissolved O_2 and the use of a conical flask created a high nitrogen, low oxygen micro-environment coupled with a small surface to reduce atmospheric oxygen exchange. Muscles dissected from the right-hand side, with their respective nerve stumps, were subject to 2 h of hypoxia (immersion in the hypoxic HEPES buffered saline) followed by 2 h reperfusion in 95% : 5% O_2 : CO_2 sparged Krebs' solution. Control muscles from the left-hand side of the same animals were maintained as experimental specimens but in 95% : 5% O_2 : CO_2 sparged Krebs' solution for the duration of the experiment (4 h). All muscles were left free floating in the conical flask with sufficient flux so as not to become stagnant but to remain below the surface during the course of the experiment.

Measurement of O_2, pH and temperature

A micro-oxygen electrode (MLT1120, AD Instruments) underwent two-point (0% and 21%) calibration in ~40 mL of distilled water placed on a magnetic stirring platform prior to each experiment. For 21%, the distilled water was left on the stirring platform for > 15 min to ensure it was fully equilibrated with atmospheric oxygen levels while 0% O_2 solution was saturated with an excess of sodium sulphite. Temperature was monitored via a probe and a temperature controller unit (TC-202A, Harvard Apparatus). Both O_2 and temperature measurements were recorded using a MacLab and Chart 4 system (AD Instruments). pH was monitored with a combination pH meter (Thermo Russel).

Immunohistochemistry

At the end of the experiment, post-synaptic acetylcholine receptors were labelled by incubation in TRITC-conjugated α-bungarotoxin (αBTX) for 10 min (5 μg mL^{-1} in oxygenated Krebs' solution: Invitrogen), prior to immersion in absolute methanol at –20 °C for 15 min. Tissues were washed in phosphate-buffered saline (PBS, Sigma) and immersed in a blocking solution [0.1% TX-100, 0.2% IgG/protease free bovine serum albumin (Jackson ImmunoResearch), 0.1% sodium azide in PBS] for a minimum of 1 h. This was followed by at least 16 h incubation with monoclonal anti-neurofilament (NF) 165 kDa primary antibodies (1 : 250) made up in blocking solution (Developmental Studies Hybridoma Bank, IA, USA) at 4 °C. This was followed by 3 × 10-min washes in PBS and a subsequent 1 h incubation in Cyanine2 (Cy2) donkey anti-mouse secondary antibodies (1 : 500, Jackson ImmunoResearch) made up in blocking solution. Following 3 × 20 min wash in PBS, the process as above was repeated but with anti-synaptic vesicle protein 2 (SV2) primary antibodies (1 : 250: Developmental Studies Hybridoma Bank, IA, USA). Following the final wash in PBS, muscles were mounted on to glass slides in 4% n-propylgallate in glycerol and stored in the dark at 4 °C.

Functional studies with FM-143FX

To assess the functional state of motor nerve terminals after hypoxia–reperfusion injury, fresh *transversus abdominis* (TA) and *triangularis sterni* (TS) muscle preparations were exposed to the

fixable analogue of the styryl dye FM-143 (FM1–43FX, 1 mg mL^{-1}: Molecular Probes) in 95% : 5% O_2 : CO_2 sparged, high K^+ Krebs' solution (102 mM Na^+, 50 mM K^+, 2 mM Ca^{2+}, 2 mM Mg^{2+}, 132 mM Cl^-, 23.8 mM HCO^{3-}, 0.4 mM $H_2PO_4^{2-}$, 5 mM D-glucose, 5.5 mM HEPES: pH 7.2–7.4) for 15 min at the end of the experiment (Betz & Bewick, 1992; Adalbert et al. 2005). Preparations were briefly rinsed in fresh Krebs' solution before fixation in 4% formaldehyde/PBS solution (Electron Microscopy Science, PA, USA) for 30 min. Postsynaptic acetylcholine receptors at the motor endplate were labelled by incubation in 5 μg mL^{-1} (in PBS) Alexa647-conjugated α-bungarotoxin (Invitrogen) for 30 min. Muscles were then washed 2 × 10 min and 2 × 15 min in PBS prior to mounting on glass slides as above.

Image capture, quantification and statistical analysis

All preparations were examined and quantified on an upright Zeiss microscope (×25, 0.6 NA water immersion objective) equipped with epifluorescence FITC/TRITC filter sets. Images from the microscope were captured via a monochrome Cohu 4910 CCD camera running Scion Image capture software (Alrad, UK). Image capture was also carried out on BioRad Radiance 2000 confocal microscope (×40, 0.8 NA oil-immersion objective) using Lasersharp 2000 software. All images had minor adjustments for brightness and contrast, and were pseudocolored as required using Abode Photoshop CS2 software.

All quantification of NF/SV2 labelled muscles was carried out at ×25 magnification and data from the four deep lumbricals were pooled. Muscles were assessed for muscle fibre integrity and any preparations with significant numbers of dead muscle fibres were excluded from further examination. Endplates were then census quantified right to left through the depth of the muscle with the following exclusions: endplate was facing away from the plane of view or belonged to a muscle fibre which lacked striations or had significant autofluorescence. Nerve terminals opposing each endplate were assessed and categorized as follows:

'*Full*': NF/SV2 immunoreactivity detected in all nerve terminal boutons that opposed the muscle endplate.

'*Partial*': NF/SV2 immunoreactivity could not be detected in one or more nerve terminal boutons opposing the muscle endplate.

'*Vacant*': No clearly distinguishable NF/SV2 immunoreactivity could be detected opposing the muscle endplate.

All data were collected using Microsoft Excel software and statistical tests were undertaken using GraphPad Prism software. All values are percentage mean ± SE, *N* = number of muscles, *n* = number of endplates.

Results

Developing a robust *ex vivo* model of hypoxia–reperfusion

To develop a robust *ex vivo* model of hypoxia–reperfusion, we generated a system in which *ex vivo* nerve/muscle preparations could be monitored and maintained in a consistent hypoxic environment with oxygen concentration below the normoxic *in vivo* values of skeletal muscle [estimated to be 0.5–5% (4–35 mmHg): Gorczynski & Duling, 1978; Honig & Gayeski, 1993; Eu et al. 2003; Matsumoto et al. 2005]. By reducing the surface area to volume ratio of the perfusate via use of a conical flask and vigorously sparging with 95% : 5% N_2 : CO_2 gas we increased displacement of already dissolved O_2 in the perfusate and created a low O_2 environment at the surface to reduce atmospheric oxygen exchange. This consistently produced an O_2 concentration below 0.25%, which is significantly below *in vivo* normoxia (Fig. 1) and similar to levels induced by tourniquet (Matsumoto et al. 2005). While hypoxic conditions were often reached within 15–30 min after sparging began, it would occasionally take up to 1.25 h for the O_2 levels to fall to a steady state. To ensure that all experiments were carried out at a consistent O_2 level, the system was allowed to equilibrate for a minimum of 1.5 h prior to being used to induce hypoxia in *ex vivo* muscle preparations. This system also allowed us to ensure that no significant changes in pH or temperature occurred during the course of the experiments.

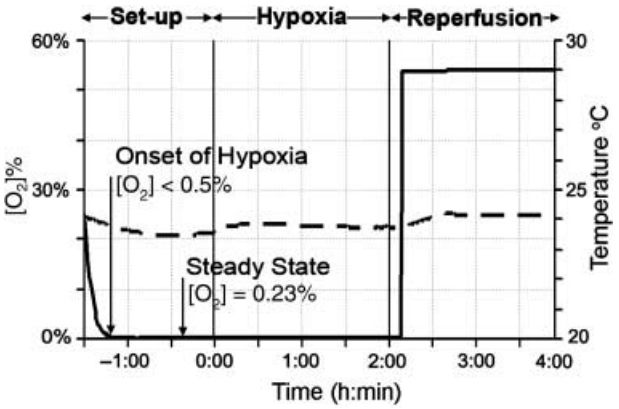

Fig. 1 Example recording showing O_2 concentration (solid line) during the system set-up phase and the experimental phases of hypoxia and reperfusion. In the set-up phase, 250 mL of Krebs' solution is sparged with 95% : 5% N_2 : CO_2 gas and O_2 concentration is seen to quickly fall in the first 15 min to less than 0.5%, which is the lowest suggested threshold for normoxia. The O_2 concentration, however, could continue to fall for a further 1 h until it reached a consistent, steady state. In all experiments where recordings took place, steady O_2 state was below 0.25% and in this example recording, was 0.23%. To ensure that oxygen levels remained constant, all hypoxia–reperfusion experiments began after the Krebs' solution was sparged with 95% : 5% N_2 : CO_2 for 1.5 h (system set-up phase). After the set-up phase, skeletal muscle preparations were added to the Krebs' solution to begin the hypoxia phase, which lasted for 2 h. This was followed by 2 h reperfusion using 95% : 5% O_2 : CO_2 gas, after which preparations were removed and processed for fluorescent staining. Temperature was monitored throughout the experiments and was maintained at 23–24 °C (hashed line). pH was also monitored throughout the experiments and was maintained between pH 7.2 and 7.4 (not shown). Control muscles were maintained in 250 mL Krebs' solution sparged only with 95 : 5% O_2 : CO_2 gas for the full 4-h duration.

Rapid loss of motor nerve terminals following hypoxia–reperfusion injury

First, we examined the effects of 2 h hypoxia followed by 2 h reperfusion (2H-2R) on the morphology of pre- and

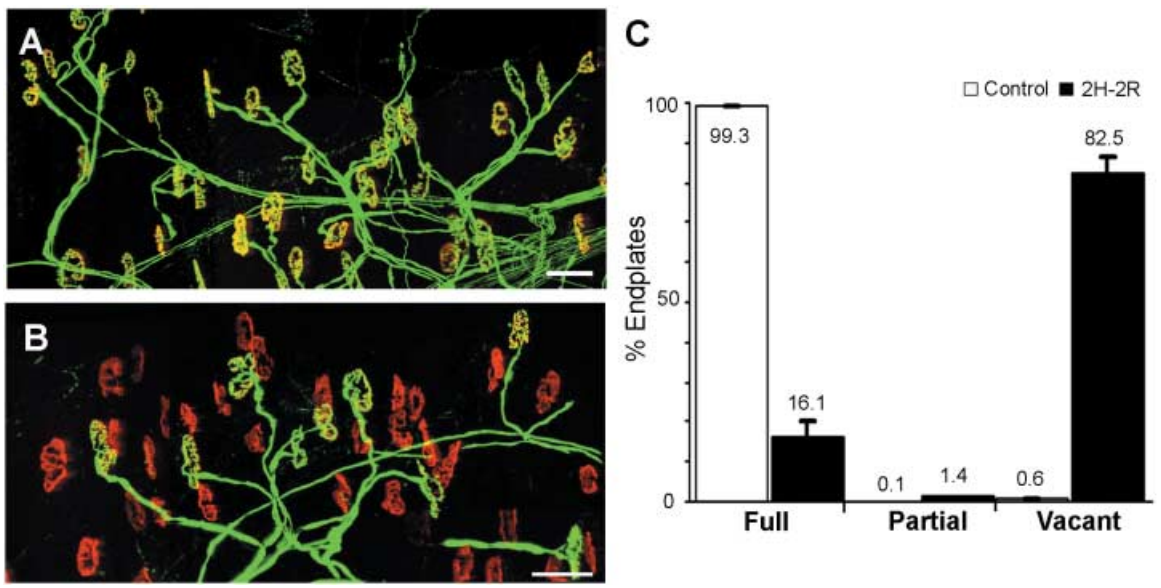

Fig. 2 2H-2R leads to rapid loss of motor nerve terminal morphology in mouse lumbrical muscles. (A,B) Confocal projections of lumbrical muscles labelled with neurofilament 165 kDa (NF) and synaptic vesicle (SV2) primary antibodies, visualized with Cy2 secondary antibodies (green). Postsynaptic muscle fibre endplates were visualized with TRITC-conjugated αBTX (red). In control conditions (A) postsynaptic endplates (red) were all fully occupied by overlying motor nerve terminals (green). Following 2H-2R, a significant proportion of postsynaptic endplates had lost pre-synaptic nerve terminals [evidenced by absence of NF/SV2 immunoreactivity; (B)]. (C) Bar chart (mean ± SE) showing quantification of nerve terminal status (e.g. fully occupied, partially occupied or vacant; see methods) in lumbrical muscles from hypoxia–reperfusion treated (2H-2R: black bars) and control (white bars) preparations. Scale bar ~50 μm.

post-synaptic components of the mouse neuromuscular junction in the four deep lumbrical muscles ($N = 28$, $n = 4974$). 2H-2R caused 82.51 ± 4.16% of motor nerve terminals to appear 'vacant' due to the loss of 165-kDa neurofilament and synaptic vesicle protein immunoreactivity from motor nerve terminal arborizations and pre-terminal axons (Fig. 2). The remaining endplates either appeared to have 'full' (16.14 ± 0.31%) or 'partial' (1.35 ± 4.02%) innervation by nerve terminal boutons (Figs 2 and 3). This dramatic and rapid change of protein immunoreactivity strongly indicates loss of integral nerve terminal morphology. This loss of morphology was in stark contrast to nerve terminals from control lumbrical muscles where 99.3 ± 0.11% of endplates were fully occupied and only a small number of endplates appeared vacant (0.57 ± 0.15%) or partially (0.1 ± 0.06%) occupied ($N = 28$, $n = 5090$) (see methods). No changes were noted in the muscle fibres or their motor endplates (determined by the presence of striations, autofluorescence and endplate integrity/morphology), in agreement with previous *in vivo* studies (Tombol et al. 2002).

Ongoing nerve terminal disassembly following hypoxia–reperfusion injury

Partially occupied neuromuscular junctions were very rarely observed in control preparations but were readily identified in 2H-2R preparations (see above), offering an ideal opportunity to examine synapses at 'intermediate' stages of breakdown, providing possible insights into the cellular pathways responsible for nerve terminal loss (Fig. 3). Examination of this subpopulation of neuromuscular junctions revealed a heterogeneous set of morphological responses. Some partially occupied endplates had lost part of their overlying nerve terminal but their incoming pre-terminal axon remained intact, indicative of a withdrawal or retraction process (Fig. 3B; Gillingwater et al. 2002; Gillingwater & Ribchester, 2003; Walsh & Lichtman, 2003; Bettini et al. 2007). Other partially occupied endplates had isolated fragments disconnected from each other and/or their pre-terminal axon (Fig. 3A,C).

Inter-muscular differences in the synaptic response to hypoxia–reperfusion injury

To investigate whether there were muscle-specific differences in hypoxia–reperfusion injury, we repeated the above experiments using TA (*transversus abdominis*) and TS (*triangularis sterni*) from the deep surface of the abdominal and thoracic walls, respectively, and compared the response with data from lumbrical muscles (L: Fig. 4). TA muscles showed a noticeable but non-significant decrease in numbers of vacant endplates (57.8 ± 11.44%), whereas TS showed a very significant decrease in the number of vacant endplates (27.7 ± 7.77%) compared with lumbrical muscles (82.51 ± 4.16%: $P < 0.01$ Kruskal-Wallis test with Dunn's *Post-hoc* test). The nerve terminals from 37.3 ± 11.93%

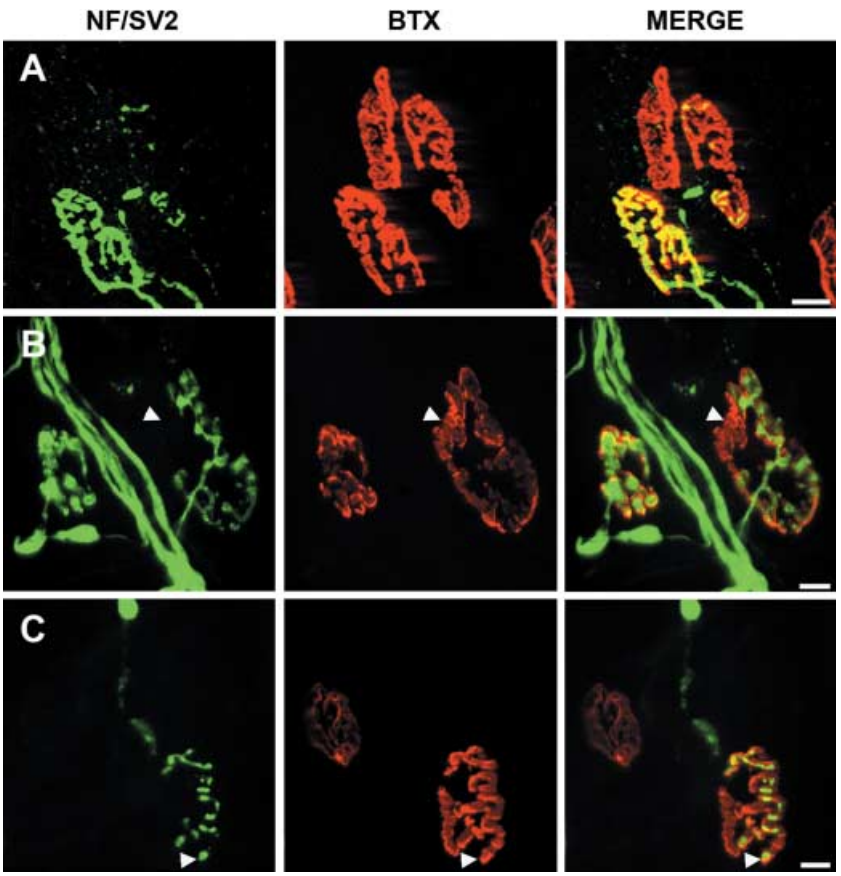

Fig. 3 Partially occupied endplates provide morphological insights into mechanisms of nerve terminal loss following hypoxia–reperfusion injury. (A) Confocal micrographs showing immunohistochemically labelled neuromuscular junctions in a lumbrical muscle following 2H-2R treatment. One endplate (red) remained fully occupied (bottom left) with 'full' overlying NF/SV2 immunoreactivity (green). A neighbouring endplate (upper middle; less than 50 μm away) had no residual NF/SV2 immunoreactivity (vacant). A third endplate (upper right) was partially occupied by overlying NF/SV2 immunoreactivity. However, note how the pre-synaptic staining is fragmented in both the motor nerve terminal and pre-terminal axon. (B) Micrograph showing another example of a partially occupied endplate (white arrowhead), which remains entirely connected to its incoming pre-terminal axon (i.e. no fragmentation). (C) Micrograph showing another example of a partially occupied endplate with fragmented morphology. Loss of NF/SV2 immunoreactivity was accompanied by numerous isolated nerve terminal fragments (arrowhead) and weak NF staining in the pre-terminal axon. Scale bar ~10 μm.

and 69 ± 8.64% of TA and TS muscles, respectively, retained a full terminal morphology compared with only 16.1% from lumbrical muscles. Interestingly, there was also an increase in the number of partially occupied endplates in the TA and TS muscles, 4.8 ± 0.76% and 3.2 ± 1.21%, respectively (TA: $N = 4$, $n = 1753$, TS: $N = 4$, $n = 1765$). Again, this is in stark contrast to control preparations, where 100% and 99.8 ± 0.02% of endplates in TA and TS, respectively, appeared fully occupied (TA: $N = 3$, $n = 2123$, TS: $N = 3$, $n = 2069$). Thus TS, and to a lesser extent TA, muscles (both predominantly slow-twitch muscle fibre type) were either more resistant to and/or slower to respond to 2H-2R treatment when compared to the predominantly fast-twitch lumbrical muscles.

Reduced vesicle recycling at the NMJ following hypoxia/reperfusion injury

Our immunocytochemical data suggested disruption of proteins related to synaptic vesicles (SV2). We therefore examined the functional consequences of 2H-2R in nerve terminals from TA and TS muscles using the vital dye FM143FX. This styryl dye becomes incorporated into synaptic vesicle membranes as they are recycled following a depolarizing stimulus (Betz & Bewick, 1992; Adalbert et al. 2005). We stimulated TA ($n = 2$) and TS ($n = 2$) muscles following 2H-2R in high K^+ Krebs' solution to load synaptic terminals with the dye (Adalbert et al. 2005: Fig. 5). No nerve terminals from 2H-2R treated muscles with clear FM1-43FX fluorescence were identified. By contrast, in control preparations > 95% of terminals examined showed clear FM1-43FX fluorescence. This suggests that 2H-2R treated terminals have a significantly reduced ability to recycle synaptic vesicles. Compared with the immunohistochemical data where TA and TS showed 57.8% and 27.7% loss in immunoreactivity, respectively, these data suggest that functional disruption may occur prior to the morphological changes shown by NF/SV2 staining.

Age-dependent changes in hypoxia–reperfusion injury

Next, we used our model to explore potential age-related differences in nerve terminal response to 2H-2R injury. Using lumbrical, TA and TS muscles, we compared nerve terminal pathology following 2H-2R in tissue from juvenile mice aged 5–6 weeks compared with adult mice aged 8–12 weeks. Nerve terminal loss in the TA and TS muscles was significantly increased in the younger mice, with 99.45 ± 0.23% and 97.29 ± 1.41% of endplates appearing vacant, respectively (Fig. 6). Perhaps due to the marked increase in vacant endplates, only 0.4 ± 0.1% and 1.3 ± 0.66% of endplates in TA and TS muscles appeared partially occupied, respectively

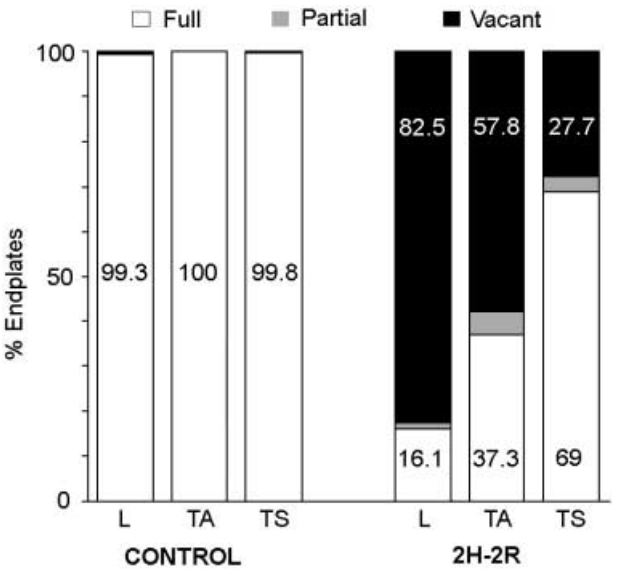

Fig. 4 Differences in nerve terminal vulnerability between skeletal muscles in response to hypoxia–reperfusion injury. Data from Fig. 2 were compared with data collected in an identical manner from two muscles taken from the abdominal and thoracic walls [*transversus abdominis* (TA) and *triangularis sterni* (TS), respectively]. The bar chart shows the quantification of endplates with a vacant (black), partial (grey) and full (white) nerve terminal morphology in lumbrical (L), TA and TS muscles under control conditions and in response to 2H-2R (error bars not shown but see results for SE). TA and TS muscles show a decreased response to 2H-2R compared with lumbrical muscles, with a greater number of endplates with a full nerve terminal morphology. Statistical comparison (Kruskal-Wallis test with Dunn's *Post-hoc* test) indicates that although the differences between the number of vacant endplates in lumbrical and TA muscles was not significant, there was a very significant decrease in the number of vacant endplates in TS muscles compared with lumbrical muscles ($P < 0.001$). This suggests that TS, and possibly also TA, muscles have an increased resistance to and/or are slower to respond to hypoxia–reperfusion injury compared with lumbrical muscles (L).

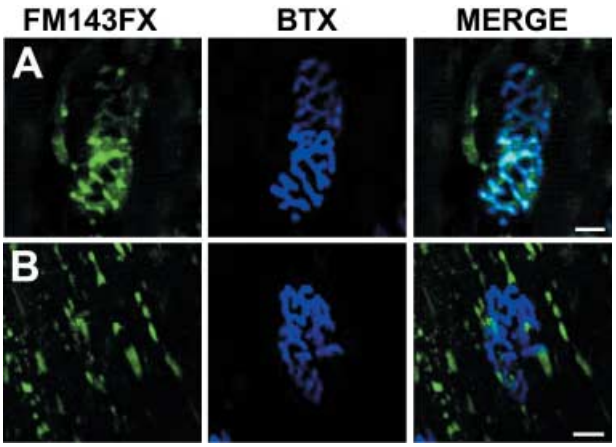

Fig. 5 Rapid loss of nerve terminal function following 2H-2R treatment. In control conditions (A) nerve terminals from the TS (shown) and TA muscles were all loaded with FM1-43FX (green) following a high K^+ depolarization stimulus. After 2H-2R (B) no nerve terminals could be found with clear FM1-43FX staining after depolarization, indicating a failure of synaptic vesicle release and recycling. Scale bar ~10 μm.

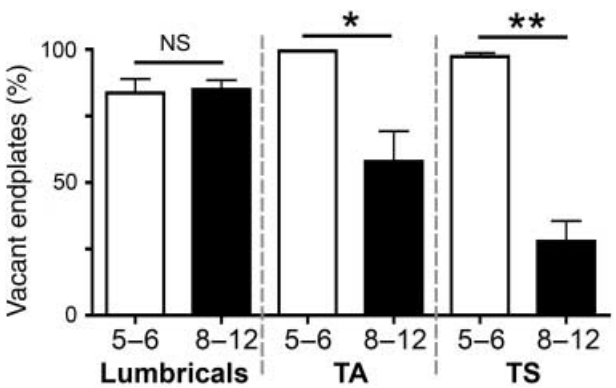

Fig. 6 Nerve terminal vulnerability to hypoxia–reperfusion injury has an age-dependent component in TA and TS muscles. Bar chart showing quantification of vacant endplates from the lumbrical, TA and TS muscles from 5–6-week-old (white bars) and 8–12-week- old (black bars) mice following 2H-2R treatment (mean ± SE). There was no significant difference in the response of lumbrical muscles from 5–6-week vs. 8–12-week-old mice ($P > 0.05$: Kruskal–Wallis test with Dunn's *Post-hoc* test). There was a significant age-dependent decrease in vulnerability of TA (*$P < 0.05$) and TS (**$P < 0.001$) muscles in 8–12-week-old mice compared with 5–6-week-old mice.

($N = 4$, TA: $n = 2104$, TS: $n = 2220$). Surprisingly, these age-related differences in vulnerability were not present in lumbrical muscles (Fig. 6), where 82.8 ± 4.34% of endplates appeared vacant in younger mice ($N = 16$, $n = 3697$). Again this was in contrast to control preparations from younger mice, where less than 1% of endplates from lumbrical ($N = 12$, $n = 2558$), TA and TS ($N = 3$, TA: $n = 1381$, TS: $n = 1921$), respectively, showed either a partial or vacant nerve terminal morphology. This suggests significant age-dependent changes in nerve terminal vulnerability to hypoxia–reperfusion injury and supports the finding of significant levels of inter-muscular variability.

Nerve terminal disassembly following hypoxia–reperfusion injury does not occur via Wallerian degeneration

Finally, we carried out experiments to determine whether motor nerve terminals were being lost by Wallerian degeneration pathways, which was suggested by the presence of fragmented nerve terminals in previous experiments. We quantified the nerve terminal response to 2H-2R in lumbrical, TA and TS muscles from mice carrying the naturally occurring *Wld*^{S} mutation. The *Wld*^{S} mutation significantly delays Wallerian degeneration of axons and nerve terminals in both the CNS and the PNS (Lunn et al. 1989; Ribchester et al. 1995; Gillingwater et al. 2003, 2006a,b; Wishart et al. 2007). As protection of nerve terminals after injury has previously been shown to weaken in *Wld*^{S} mice from 4 months of age onwards (Gillingwater et al. 2002), we ensured strong synaptic protection by

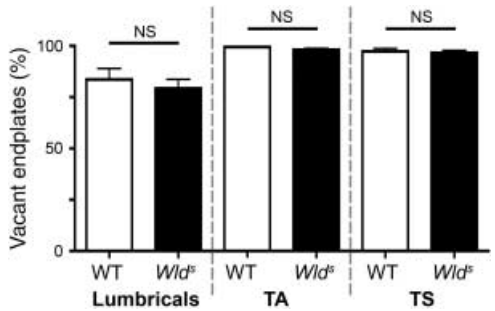

Fig. 7 Hypoxia–reperfusion injury was not modified by the *Wld*^{S} mutation. Bar chart showing quantification of vacant endplates from the lumbrical, TA and TS muscles from 5–6-week-old wild-type (WT) and *Wld*^{S} mice following 2H-2R treatment (mean ± SE). The *Wld*^{S} mutation had no significant neuroprotective effect following hypoxia–reperfusion injury in all muscles examined ($P > 0.05$ for all muscles examined, Kruskal-Wallis test with Dunn's *Post-hoc* test).

using muscles from animals at 5–6 weeks of age. Compared to wild-type animals of a similar age (as detailed above), the *Wld*^{S} mutation conveyed no significant ($P > 0.05$) neuroprotective effect on motor nerve terminals in lumbrical, TA or TS muscles in response to 2H-2R (Fig. 7). For *Wld*^{S} muscles, values for vacant endplates appearing with no NF/SV2 immunoreactivity were as follows: lumbrical muscles 82.4 ± 2.88% ($N = 24$, $n = 5468$), TA 98 ± 0.71% ($N = 5$, $n = 2568$) TS 96.64 ± 1.15% ($N = 5$, $n = 2290$). This contrasts with control preparations from *Wld*^{S} mice (not shown), where less than 1.5% of endplates from lumbrical ($N = 12$, $n = 2718$), TA ($N = 3$, $n = 1934$) and TS ($N = 3$, $n = 1894$) showed either a partial or vacant nerve terminal morphology. The failure of *Wld*^{S} to protect motor nerve terminals against 2H-2R injury suggests that nerve terminal disassembly is occurring via mechanisms distinct from classic Wallerian degeneration.

Discussion

We present morphological and functional evidence showing that mouse motor nerve terminals are vulnerable to hypoxia–reperfusion injury. Using a novel *ex vivo* model system where O_2 concentration was maintained consistently below *in vivo* normoxic values and at a level similar to that induced by tourniquet (Gorczynski & Duling, 1978; Honig & Gayeski, 1993; Eu et al. 2003; Matsumoto et al. 2005), we have shown that in response to 2 h hypoxia–2 h reperfusion (2H-2R) neurofilament and synaptic vesicle immunoreactivity was rapidly lost from the majority of motor nerve terminals and pre-terminal axons. The severity of synaptic pathology was dependent on the age of the mouse and muscle type. Our study demonstrates that hypoxia–reperfusion injury is a major pathological stimulus at motor nerve terminals and therefore is likely to contribute significantly towards the neurological damage routinely induced by tourniquets.

Loss of neurofilament and synaptic vesicle proteins was preceded by functional disruption, manifested as a failure to release and recycle synaptic vesicles. Similar functional responses have been observed in CNS ischaemia (for reviews see e.g. Lipton, 1999, White et al. 2000), including reduced synaptic transmission, reduced synaptic vesicle density (Kovalenko et al. 2006) and a loss of pre-synaptic proteins critical for regulating synaptic vesicle turnover (Ishimaru et al. 2001). Similar temporal changes in function and morphology are known to occur in other neurodegenerative processes, including Wallerian degeneration and motor neuron disease (Miledi & Slater, 1970; Miura et al. 1993; Ferri et al. 2003; Gillingwater & Ribchester, 2003; Pun et al. 2006; Wishart et al. 2006; Murray et al. 2008). Despite some morphological similarities, the data show that nerve terminal loss following hypoxia–reperfusion injury does not occur via Wallerian degeneration, as the Wallerian degeneration slow (*Wld*^{S}) gene failed to protect nerve terminals from 2H-2R. Further investigations of the mechanism(s) responsible for disassembling motor nerve terminals following hypoxia–reperfusion injury are therefore required and will benefit from using the experimentally accessible *ex vivo* methodology developed in the current study.

Recent *in vivo* studies documenting the morphological vulnerability of motor nerve terminals to ischaemia–reperfusion injury have utilized elasticated rubber bands as tourniquets (Tombol et al. 2002; David et al. 2007), which undoubtedly cause mechanical stress alongside hypoxia/ischaemia. As a result, they have been unable conclusively to distinguish between the contribution of mechanically induced degeneration, known to occur in response to nerve crush, (Ochoa et al. 1972; Beirowski et al. 2005) and the effects of ischaemia–reperfusion. Furthermore, these studies have been unable to distinguish between the relative importance of inflammation, acidosis or gross biochemical/ionic changes that may occur when using tourniquet and their contribution to injury (see e.g. Rorabeck, 1980 or for review Kam et al. 2001). In our *ex vivo* model of hypoxia–reperfusion injury we are able to show clearly that changes in oxygen tension alone are a major pathological stimulus for motor nerve terminals, which is capable of inducing rapid changes in nerve terminal form and function.

The data presented here demonstrate that the extent of motor nerve terminal injury in response to hypoxia–reperfusion injury depends on the age of the animal and muscle location/type. When we compared the effects of 2H-2R on predominantly slow-fibre type muscles (TA and TS) with that on predominantly fast-fibre type muscles (lumbricals) we identified significant differences in vulnerability, with the lumbricals more affected than TA or TS. Similarly, when we compared the response of muscles from 5–6-week and 8–12-week-old mice, TA and TS muscles from older animals were significantly less vulnerable to 2H-2R than muscles from younger animals. These findings

suggest that different populations of neuromuscular nerve terminals, with characteristics determined by their level of maturity, muscle fibre type and/or location within the body, have distinct levels of vulnerability/resistance to hypoxia–reperfusion injury. David et al. (2007) and Tombol et al. (2002) have recently reported that nerve terminals from slow-twitch muscles are more resistant to ischaemia–reperfusion injury, whereas Chervu et al. (1989) report that slow-twitch muscles are more susceptible. Our experiments suggest that nerve terminals on slow-twitch muscle fibres are more resistant to hypoxia–reperfusion injury than those on fast-twitch fibres, at least in more mature animals. Selective vulnerability within populations of neurons have also been reported following cerebral ischemia in the CNS (Lipton, 1999) and there is a growing body of evidence suggesting that certain motor unit characteristics confer selective vulnerability/resistance in a range of neurodegenerative conditions, such as motor neuron disease (Frey et al. 2000; Schaefer et al. 2005; Pun et al. 2006; Murray et al. 2008). However, the reasons underlying such a rapid age-dependent switch in synaptic vulnerability remain unclear. These mechanisms are likely to be important to understand the cellular pathways that regulate synaptic vulnerability. Our model system may provide an ideal tool with which to examine these mechanisms and pathways.

The failure of the *Wld*^{s} gene to protect against nerve terminal loss following hypoxia–reperfusion injury suggests that mechanisms distinct from classic Wallerian degeneration are being activated. The heterogeneous range of morphological responses observed at nerve terminals following hypoxia–reperfusion injury (Fig. 3) suggests that multiple mechanisms may be involved. These observations are supported by previous studies from the CNS where up to four simultaneous morphological phenotypes of ischaemic neuronal loss have been identified (for review see Lipton, 1999). We identified nerve terminal morphologies indicative of Wallerian-like fragmentation processes as well as asynchronous nerve terminal retraction. Although nerve terminal retraction is normally a mechanism of loss associated with developmental synapse elimination (Sanes & Lichtman, 1999; Keller-Peck et al. 2001; Gillingwater et al. 2002; Gillingwater & Ribchester, 2003; Walsh & Lichtman, 2003; Parson et al. 2004), there are increasing numbers of reports showing that withdrawal can occur in response to injury and disease in adult motor nerve terminals (Gillingwater et al. 2002; Fischer et al. 2004; Bettini et al. 2007; Murray et al. 2008). The finding that nerve terminal function may be disrupted in advance of disassembly suggests that future experiments are required to define accurately the spatio-temporal characteristics of hypoxia–reperfusion injury. The combination of a broader spectrum of immunocytochemical markers (labelling a range of different membranous, cytoskeletal and vesicular proteins) combined with functional analyses (e.g. electrophysiology) and ultrastructural analyses would be required.

In summary, we have shown that motor nerve terminals are vulnerable to hypoxia–reperfusion injury. This is of important clinical significance as hypoxia is induced during application of tourniquets and during a range of disease processes. We have developed a novel, robust, experimentally accessible *ex vivo* model of hypoxia–reperfusion injury which we have used to identify differences in nerve terminal vulnerability between individual muscles and in mice of different ages. We have also used the model to demonstrate that nerve terminal loss following hypoxia–reperfusion injury occurs via mechanisms distinct from Wallerian degeneration.

Acknowledgements

Grant numbers/sources of support: The authors gratefully acknowledge financial support from the Anatomical Society of Great Britain and Ireland (B.B., T.H.G., S.H.P.), Medical Research Scotland (T.H.G.) and the BBSRC (T.H.G.).

References

Adalbert R, Gillingwater TH, Haley JE, et al. (2005) A rat model of slow Wallerian degeneration (WldS) with improved preservation of neuromuscular synapses. *Eur J Neurosci* **21**, 271–277.

Beirowski B, Adalbert R, Wagner D, et al. (2005) The progressive nature of Wallerian degeneration in wild-type and slow Wallerian degeneration (WldS) nerves. *BMC Neurosci* **6**, 6.

Bettini NL, Moores TS, Baxter B, Deuchars J, Parson SH (2007) Dynamic remodelling of synapses can occur in the absence of the parent cell body. *BMC Neurosci* **8**, 79.

Betz WJ, Bewick GS (1992) Optical analysis of synaptic vesicle recycling at the frog neuromuscular junction. *Science* **255**, 200–203.

Bickler PE, Donohoe PH (2002) Adaptive responses of vertebrate neurons to hypoxia. *J Exp Biol* **205**, 3579–3586.

Bukharaeva EA, Salakhutdinov RI, Vyskocil F, Nikolsky EE (2005) Spontaneous quantal and non-quantal release of acetylcholine at mouse endplate during onset of hypoxia. *Physiol Res* **54**, 251–255.

Chervu A, Moore WS, Homsher E, Quinones-Baldrich WJ (1989) Differential recovery of skeletal muscle and peripheral nerve function after ischemia and reperfusion. *J Surg Res* **47**, 12–19.

David G, Nguyen K, Barrett EF (2007) Early vulnerability to ischemia/reperfusion injury in motor terminals innervating fast muscles of SOD1-G93A mice. *Exp Neurol* **204**, 411–420.

Eastlack RK, Groppo ER, Hargens AR, Pedowitz RA (2004) Ischemic-preconditioning does not prevent neuromuscular dysfunction after ischemia-reperfusion injury. *J Orthop Res* **22**, 918–923.

Eu JP, Hare JM, Hess DT, et al. (2003) Concerted regulation of skeletal muscle contractility by oxygen tension and endogenous nitric oxide. *Proc Natl Acad Sci U S A* **100**, 15229–15234.

Ferri A, Sanes JR, Coleman MP, Cunningham JM, Kato AC (2003) Inhibiting axon degeneration and synapse loss attenuates apoptosis and disease progression in a mouse model of motoneuron disease. *Curr Biol* **13**, 669–673.

Fischer LR, Culver DG, Tennant P, et al. (2004) Amyotrophic lateral sclerosis is a distal axonopathy: evidence in mice and man. *Exp Neurol* **185**, 232–240.

Frey D, Schneider C, Xu L, Borg J, Spooren W, Caroni P (2000) Early and selective loss of neuromuscular synapse subtypes with low

sprouting competence in motoneuron diseases. *J Neurosci* **20**, 2534–2542.

Gillingwater TH, Ribchester RR (2003) The relationship of neuromuscular synapse elimination to synaptic degeneration and pathology: insights from WldS and other mutant mice. *J Neurocytol* **32**, 863–881.

Gillingwater TH, Thomson D, Mack TGA, et al. (2002) Age-dependent synapse withdrawal at axotomised neuromuscular junctions in Wlds mutant and Ube4b/Nmnat transgenic mice. *J Physiol (Lond)* **543**, 739–755.

Gillingwater TH, Ingham CA, Coleman MP, Ribchester RR (2003) Ultrastructural correlates of synapse withdrawal at axotomized neuromuscular junctions in mutant and transgenic mice expressing the Wld gene. *J Anat* **203**, 265–276.

Gillingwater TH, Ingham CA, Parry KE, et al. (2006a) Delayed synaptic degeneration in the CNS of Wlds mice after cortical lesion. *Brain* **129**, 1546–1556.

Gillingwater TH, Wishart TM, Chen PE, et al. (2006b) The neuroprotective WldS gene regulates expression of PTTG1 and erythroid differentiation regulator 1-like gene in mice and human cells. *Hum Mol Genet* **15**, 625–635.

Gorczynski RJ, Duling BR (1978) Role of oxygen in arteriolar functional vasodilation in hamster striated muscle. *Am J Physiol* **235**, H505–515.

Hatzipantelis KP, Natsis K, Albani M (2001) Effect of acute limb ischaemia on neuromuscular function in rats. *Eur J Surg* **167**, 831–838.

Honig CR, Gayeski TE (1993) Resistance to O_2 diffusion in anemic red muscle: roles of flux density and cell PO_2. *Am J Physiol* **265**, H868–875.

Ishimaru H, Casamenti F, Ueda K, Maruyama Y, Pepeu G (2001) Changes in presynaptic proteins, SNAP-25 and synaptophysin, in the hippocampal CA1 area in ischemic gerbils. *Brain Res* **903**, 94–101.

Kam PCA, Kavanaugh R, Yoong FFY (2001) The arterial tourniquet: pathophysiological consequences and anaesthetic implications. *Anaesthesia* **56**, 534–545.

Keller-Peck CR, Walsh MK, Gan WB, Feng G, Sanes JR, Lichtman JW (2001) Asynchronous synapse elimination in neonatal motor units: studies using GFP transgenic mice. *Neuron* **31**, 381–394.

Kovalenko T, Osadchenko I, Nikonenko A, et al. (2006) Ischemia-induced modifications in hippocampal CA1 stratum radiatum excitatory synapses. *Hippocampus* **16**, 814–825.

Lipton P (1999) Ischemic cell death in brain neurons. *Physiol Rev* **79**, 1431–1568.

Lunn ER, Perry VH, Brown MC, Rosen H, Gordon S (1989) Absence of Wallerian degeneration does not hinder regeneration in peripheral nerve. *Eur J Neurosci* **1**, 27–33.

Makitie J, Teravainen H (1977) Ultrastructure of striated muscle of the rat after temporary ischemia. *Acta Neuropathol* **37**, 237–45.

Matsumoto A, Matsumoto S, Sowers AL, et al. (2005) Absolute oxygen tension (pO_2) in murine fatty and muscle tissue as determined by EPR. *Magn Reson Med* **54**, 1530–1535.

McEwen JA (1981) Complications of and improvements in pneumatic tourniquets used in surgery. *Med Instrum* **15**, 253–257.

McGraw RW, McEwen JA (1987) Unsatisfactory results in hand surgery: the tourniquet. In *The Hand and Upper Limb* (ed. McFarlane RM), pp. 5–13. Edinburgh: Churchill Livingstone.

Miledi R, Slater CR (1970) On the degeneration of rat neuromuscular junctions after nerve section. *J Physiol* **207**, 507–528.

Miura H, Oda K, Endo C, Yamazaki K, Shibasaki H, Kikuchi T (1993) Progressive degeneration of motor nerve terminals in GAD mutant mouse with hereditary sensory axonopathy. *Neuropathol Appl Neurobiol* **19**, 41–51.

Murray LM, Comley LH, Thomson D, Parkinson N, Talbot K, Gillingwater TH (2008) Selective vulnerability of motor neurons and dissociation of pre- and post-synaptic pathology at the neuromuscular junction in mouse models of spinal muscular atrophy. *Hum Mol Genet* **17**, 949–962.

Nishimura M (1986) Factors influencing an increase in spontaneous transmitter release by hypoxia at the mouse neuromuscular junction. *J Physiol* **372**, 303–313.

Ochoa J, Fowler TJ, Gilliatt RW (1972) Anatomical changes in peripheral nerves compressed by a pneumatic tourniquet. *J Anat* **113**, 433–455.

Ohara WM, Pedowitz RA, Oyama BK, Gershuni DH (1996) Comparison of functional deficits in the rabbit tibialis anterior following tourniquet ischemia and tourniquet compression. *J Orthop Res* **14**, 626–632.

Parson SH, Ribchester RR, Davie N, et al. (2004) Axotomy-dependent and -independent synapse elimination in organ cultures of Wld(s) mutant mouse skeletal muscle. *J Neurosci Res* **76**, 64–75.

Pun S, Santos AF, Saxena S, Xu L, Caroni P (2006) Selective vulnerability and pruning of phasic motoneuron axons in motoneuron disease alleviated by CNTF. *Nat Neurosci* **9**, 408–419.

Ribchester RR, Tsao JW, Barry JA, Asgari-Jirhandeh N, Perry VH, Brown MC (1995) Persistence of neuromuscular junctions after axotomy in mice with slow Wallerian degeneration (C57BL/Wlds). *Eur J Neurosci* **7**, 1641–1650.

Rorabeck CH (1980) Tourniquet-induced nerve ischemia: an experimental investigation. *J Trauma* **20**, 280–286.

Sanes JR, Lichtman JW (1999) Development of the vertebrate neuromuscular junction. *Ann Rev Neurosci* **22**, 389–442.

Saunders KC, Louis DL, Weingarden SI, Waylonis GW (1979) Effect of tourniquet time on postoperative quadriceps function. *Clin Orthop Relat Res* 194–199.

Schaefer AM, Sanes JR, Lichtman JW (2005) A compensatory subpopulation of motor neurons in a mouse model of amyotrophic lateral sclerosis. *J Comp Neurol* **490**, 209–219.

Tombol T, Pataki G, Nemeth A, Hamar J (2002) Ultrastructural changes of the neuromuscular junction in reperfusion injury. *Cells Tissues Organs* **170**, 139–150.

Waller A (1850) Experiments on the section of glossopharyngeal and hypoglossal nerves of the frog and observations of the alternatives produced thereby in the structure of their primitive fibres. *Philos Trans R Soc Lond B* **140**, 423–429.

Walsh MK, Lichtman JW (2003) In vivo time-lapse imaging of synaptic takeover associated with naturally occurring synapse elimination. *Neuron* **37**, 67–73.

White BC, Sullivan JM, DeGracia DJ, et al. (2000) Brain ischemia and reperfusion: molecular mechanisms of neuronal injury. *J Neurol Sci* **179**, 1–33.

Wishart TM, Parson SH, Gillingwater TH (2006) Synaptic vulnerability in neurodegenerative disease. *J Neuropathol Exp Neurol* **65**, 733–739.

Wishart TM, Paterson JM, Short DM, et al. (2007) Differential proteomics analysis of synaptic proteins identifies potential cellular targets and protein mediators of synaptic neuroprotection conferred by the slow Wallerian degeneration (Wlds) gene. *Mol Cell Proteomics* **6**, 1318–1330.